Pressure balance in a low collisionality tokamak scrape-off layer

R.M. Churchill, C.S. Chang, S. Ku, R. Hager, R. Maingi, D. Stotler, H.Qin
Princeton Plasma Physics Laboratory
Princeton, New Jersey 08540, USA
Email: rchurchi@pppl.gov

Abstract

The gyrokinetic neoclassical code XGCa finds that the parallel pressure balance in the diverted scrape-off layer does not follow that from fluid description based on the CGL theory. Here a gyrofluid equation for pressure balance in a low-collisionality tokamak SOL is derived, for use in interpreting this difference. The new pressure balance equation allows determining physical processes which dominate the setting of pressure in the divertor, utilizing closuer information directly from a kinetic code which reduces the number of assumptions going into a fluid code. This pressure balance equation is applied to a DIII-D H-mode discharge, and its found that the total pressure balance is much better matched using the gyrofluid equation. Electrons are shown to be dominantly adiabatic, while ions have multiple contributions to pressure balance, including radial fluxes due to parallel energy flow and $E \times B$ motion.

1. Introduction

Predicting scrape-off layer (SOL) divertor pressure based on upstream pressure (or vice-versa) remains a key need to ensure future fusion devices can achieve the high global pressure needed for a burning plasma while limiting the heat and particle fluxes to material surfaces to acceptable levels. More and more, complex simulation codes are being turned to with the goal of including the multiphysics needed to accurately simulate the SOL. Understanding the relative importance of various physics included in these complex simulations is a challenging but important task.

Kotov and Reiter [1] and a recent paper by Stangeby[2] recognized this need, to treat these code simulations as 'experiments', which benefit from formatting the simulation results in simple terms. This not only gives insights into the physical processes at work in the simulation, but also serves as a validation check that the code is solving the equations you've specified. These papers focused on formatting SOL fluid codes (e.g. SOLPS) outputs into two-point modelling (2PM)[3] like expressions, which relate upstream and downstream quantities such as pressure in the SOL. At its base, 2PM is simply derived from a fluid momentum balance, with a number of extensions accounting for particle/momentum/energy sources, cross-field transport, etc.[3]

A simple application of 2PM was done with code output from an XGCa simulation of a low collisionality DIII-D[4] H-mode discharge[5, 6]. The total pressure downstream did not match the simple 2PM expectations of constant total pressure along a flux surface in the SOL, particularly in the near-SOL (here total pressure refers to the static pressure plus dynamic pressure, i.e. $p_{tot} = p + mnu_{\|}^2$), see Figure 1. Simplified expressions containing a CGL viscosity approximation, and neutral source term did not resolve the discrepancy, see Figure 1 again. It was obvious a more thorough expression based on the kinetic equations of motion in XGCa was needed to determine the physics responsible.

The purpose of this paper is to derive such an expression for the pressure balance in the SOL, utilizing outputs from the XGCa code. XGCa is a gyrokinetic neoclassical code[7] (i.e. uses a gyrokinetic equation of motion[8], but only solves for the $n = 0$ potential, no turbulence), and as such has many subtleties when forming full fluid equations, due to the need for a pullback transformations on the 5D guiding-center distribution function ($f(\mathbf{R}, v_{\perp}, v_{\|}, t)$).

Indeed, previous work[9] attempting to calculate a full pressure tensor including off-diagonal terms (similar to the "pressure tensor unfolding" technique[10]) produced certain large, unbalanced terms which may require higher order terms in the Taylor expansion of the full distribution function in order to enable use. To avoid these issues, we instead in this paper focus on forming gyrofluid equations by directly taking moments of the gyrokinetic equations of motion in XGCa.

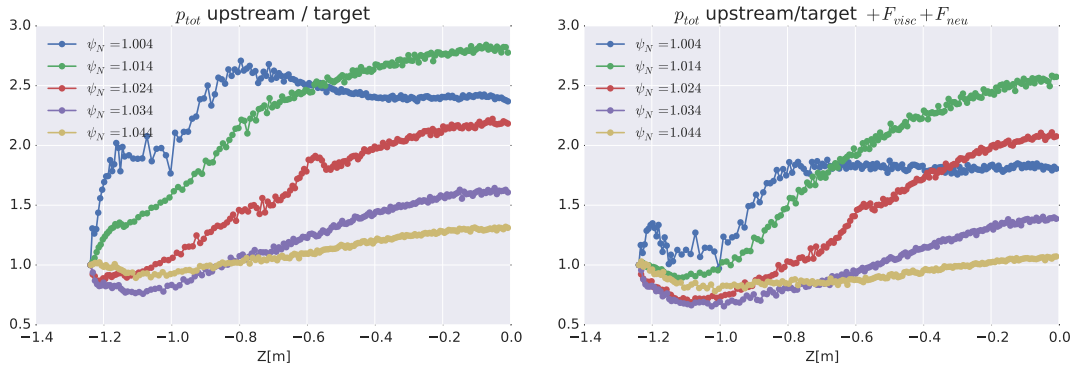

Figure 1: *Pressure balance in the SOL, plotted along flux surfaces (plotted versus Z, the normal cylindrical coordinate height coordinate, at each point on the flux surface). The left figure shows the ratio of pressure to target pressure, and the right figure shows the same but with CGL viscosity and neutral source terms added.*

2. XGCa

TODO Describe briefly XGCa, and specifically anything relevant to the current paper.

3. Gyrofluid parallel momentum equation

Gyrofluid formulations have a long history in fusion physics[11, 12, 13, 14]. The basic concept is to take moments of the gyrokinetic equation directly, and thereby derive fluid-like equations for conservation of particles, momentum, energy, etc., which still retain various kinetic effects such as finite Larmor radious (FLR) effects. Usually gyrofluid equations are used in a "predictive" fashion, where closures are selected to deal with higher order moments in the equations. Here the gyrofluid equation we derive will be used in an "interpretive" manner, where we will use the guiding-center distribution function from XGCa to calculate all moments in the gyrofluid equation, avoiding the need for closures, and allowing us to understand terms which are important in the momentum equation (and hence pressure balance).

We begin with the electrostatic gyrokinetic equations of motion used in XGCa[8]:

$$\begin{gathered}\partial_t f + \dot{\mathbf{X}}\cdot\nabla f + \dot{v}_\parallel\cdot\partial_{v_\parallel} f = S^*(f)\\ \dot{\mathbf{X}} = \tfrac{1}{D}\left[v_\parallel\hat{\mathbf{b}} + \tfrac{mv_\parallel^2}{qB}\nabla\times\hat{\mathbf{b}} + \tfrac{1}{qB^2}\mathbf{B}\times\left(\mu\nabla B - q\bar{\mathbf{E}}\right)\right]\\ \dot{v}_\parallel = -\tfrac{1}{mD}\left(\hat{\mathbf{b}} + \tfrac{mv_\parallel}{qB}\nabla\times\hat{\mathbf{b}}\right)\cdot\left(\mu\nabla B - q\bar{\mathbf{E}}\right)\\ D = 1 + \tfrac{mv_\parallel}{qB}\hat{\mathbf{b}}\cdot\left(\nabla\times\hat{\mathbf{b}}\right)\end{gathered} \tag{1}$$

Here $f = f(\mathbf{R}, v_\parallel, \mu, t)$ is the guiding-center distribution functions, S^* is a source term including collisions, neutrals, heating, etc., $\bar{\mathbf{E}} = -\overline{\nabla\Phi}$ is the gyroaveraged electric field, and other variables have their normal meaning. Note importantly that this equation was derived for a $(\mathbf{R}, v_\parallel, \mu, t)$ system, so that e.g. the ∇ operator is done holding $(v_\parallel, \mu)$ constant. For ease of taking moments of this equation, we can write in a conservative form:

$$\partial_t\left(B^* f\right) + \nabla\cdot\left(B^*\dot{\mathbf{X}} f\right) + \partial_{v_\parallel}\left(B^*\dot{v}_\parallel f\right) = B^* S(f) \tag{2}$$

where $B^* = BD$, and we have used the observation that $\partial_t B^* + \nabla\cdot\left(B^*\dot{\mathbf{X}}\right) + \partial_{v_\parallel}\left(B^*\dot{v}_\parallel\right) = 0$. We now form the gyrofluid parallel momentum equation by multiplying Equation 2 by $mv_\parallel$ and integrating over velocity space, $\int d^3v = \int dv_\parallel dv_\perp v_\perp$. After some algebra, we arrive at the desired gyrofluid parallel momentum equation:

$$\begin{gathered}\partial_t\left(mnu_\parallel\right) + \hat{\mathbf{b}}\cdot\nabla\left(p_\parallel + mnu_\parallel^2\right) - \left(\hat{\mathbf{b}}\cdot\tfrac{\nabla B}{B}\right)\left(p_\parallel + mnu_\parallel^2 - p_\perp\right) - \hat{\mathbf{b}}\cdot\left\langle q\bar{\mathbf{E}}\right\rangle_f +\\ + \tfrac{m}{qB}\left[\left(\hat{\mathbf{b}}\cdot\nabla\times\hat{\mathbf{b}}\right)\partial_t\left(p_\parallel + mnu_\parallel^2\right) + \left(\nabla\times\hat{\mathbf{b}}\right)\cdot\left(\nabla\langle mv_\parallel^3\rangle_f - \tfrac{\nabla B}{B}\langle mv_\parallel^3\rangle_f + \tfrac{\nabla B}{B}\langle mv_\parallel v_\perp^2\rangle_f - 2\langle v_\parallel q\bar{\mathbf{E}}\rangle_f\right) +\right.\\ \left. + \left(\hat{\mathbf{b}}\times\tfrac{\nabla B}{B}\right)\cdot\nabla\langle\tfrac{1}{2}mv_\parallel v_\perp^2\rangle_f + \hat{\mathbf{b}}\cdot\nabla\times\left\langle v_\parallel q\bar{\mathbf{E}}\right\rangle_f\right] = \langle mv_\parallel\rangle_S + \tfrac{m}{qB}\left(\hat{\mathbf{b}}\cdot\nabla\times\hat{\mathbf{b}}\right)\left\langle mv_\parallel^2\right\rangle_S\end{gathered} \tag{3}$$

the notation $\langle A \rangle_f = \int d\mathbf{v} A f$ is used, and the following definitions for moments:

$$\begin{array}{llll} n &= \int d\mathbf{v} f & nu_\parallel &= \int d\mathbf{v} v_\parallel f \\ p_\parallel &= \int d\mathbf{v} m (v_\parallel - u_\parallel)^2 f & p_\perp &= \int d\mathbf{v} \frac{1}{2} m v_\perp^2 f \end{array} \tag{4}$$

In order to have an expression for the pressure directly, we will performe a line integral along the parallel direction, $\int d\ell_\parallel$. Applying this integral to Eq. 2, and rearranging terms, we arrive at an equation similar to past equations[6]:

$$\frac{p_{\parallel,tot}|_{\ell_\parallel = x}}{p_{\parallel,tot}|_{\ell_\parallel = 0}} + \sum_j F_j = 1 \tag{5}$$

where we have written $p_{\parallel,tot} = p_\parallel + mnu_\parallel^2$, and where each F_j represents the integral of one of the terms from Equation 2 (excluding the parallel gradient of pressure term), normalized to $(p_{\parallel,tot}/B)|_{\ell_\parallel = 0}$. The F_j terms are as follows:

$$\begin{array}{llll} F_{\partial_t} &= \frac{-\int_0^x d\ell_\parallel \partial_t (mnu_\parallel) + \frac{m}{qB}(\hat{\mathbf{b}}\cdot\nabla\times\hat{\mathbf{b}})\partial_t(p_\parallel + mnu_\parallel^2)}{p_{\parallel,tot}|_{\ell_\parallel=0}} & F_{visc} &= \frac{-\int_0^x d\ell_\parallel (\hat{\mathbf{b}}\cdot\frac{\nabla B}{B})\left(p_\parallel + mnu_\parallel^2 - p_\perp\right)}{p_{\parallel,tot}|_{\ell_\parallel=0}} \\ F_{E_\parallel} &= \frac{-\int_0^x d\ell_\parallel \hat{\mathbf{b}}\cdot\langle\overline{\mathbf{E}}\rangle_f}{p_{\parallel,tot}|_{\ell_\parallel=0}} & F_{source} &= \frac{\int_0^x d\ell_\parallel \langle mv_\parallel\rangle_S + \frac{m}{qB}(\hat{\mathbf{b}}\cdot\nabla\times\hat{\mathbf{b}})\langle mv_\parallel^2\rangle_S}{p_{\parallel,tot}|_{\ell_\parallel=0}} \\ F_{\nabla m v_\parallel^2} &= \frac{\int_0^x d\ell_\parallel \frac{m}{qB}(\nabla\times\hat{\mathbf{b}})\cdot\nabla\langle mv_\parallel^3\rangle_f}{p_{\parallel,tot}|_{\ell_\parallel=0}} & F_{(\nabla\times\hat{\mathbf{b}})\cdot\frac{\nabla B}{B}} &= \frac{\int_0^x d\ell_\parallel \frac{m}{qB}(\nabla\times\hat{\mathbf{b}})\cdot\frac{\nabla B}{B}\left(\langle mv_\parallel v_\perp^2\rangle_f - \langle mv_\parallel^3\rangle_f\right)}{p_{\parallel,tot}|_{\ell_\parallel=0}} \\ F_{2\langle v_\parallel q\bar{\mathbf{E}}\rangle_f} &= \frac{-\int_0^x d\ell_\parallel \frac{m}{qB}(\nabla\times\hat{\mathbf{b}})\cdot 2\langle v_\parallel q\bar{\mathbf{E}}\rangle_f}{p_{\parallel,tot}|_{\ell_\parallel=0}} & F_{\nabla\langle\frac{1}{2}mv_\parallel v_\perp^2\rangle_f} &= \frac{\int_0^x d\ell_\parallel \frac{m}{qB}(\hat{\mathbf{b}}\times\frac{\nabla B}{B})\cdot\nabla\langle\frac{1}{2}mv_\parallel v_\perp^2\rangle_f}{p_{\parallel,tot}|_{\ell_\parallel=0}} \\ F_{\hat{\mathbf{b}}\cdot\nabla\times\langle v_\parallel q\bar{\mathbf{E}}\rangle_f} &= \frac{\int_0^x d\ell_\parallel \frac{m}{qB}(\hat{\mathbf{b}}\times\frac{\nabla B}{B})\cdot\hat{\mathbf{b}}\cdot\nabla\times\langle v_\parallel q\bar{\mathbf{E}}\rangle_f}{p_{\parallel,tor}|_{\ell_\parallel=0}} & & \end{array} \tag{6}$$

4. Gyrofluid pressure balance in XGCa

We now use the integrated gyrofluid momentum equation (Equation 5) with the guiding-center distribution functions, f_e and f_i, and field quantities from an XGCa simulation of a lower collisionality H-mode DIII-D discharge. This is the same discharge and simulation setup as Ref. [5], however the simulation has been redone to include additional diagnostic outputs useful for calculating Equation 5, such as the source term and gyroaveraged electric field.

The sum of electron and ion pressure and parallel momentum equation terms (the LHS of Equation 5) for a flux-surface in the near-SOL ($\psi_N = 1.002$) are plotted in Figure 2. For comparison, the total pressure normalized to the target pressure is plotted also, $\frac{p_{tot}|_{\ell_\parallel = x}}{p_{tot}|_{\ell_\parallel = 0}}$. Complete pressure balance would result in the plot being one everywhere (unity line). As seen, the gyrofluid formulation is a significant improvement, especially upstream from the divertor, within a 20-40% maximum deviation from the unity line. The main deviation is caused by the ions; the electrons are always better matched. Also, this deviation mainly comes about when including the region near the X-point. If the flux surface were split into two regions, below and above the X-point, the pressure balance is very close to the unity line. For flux surfaces further away from the X-point, the pressure balance is much closer to unity. A discussion of the remaining deviation in the near-SOL flux surfaces will be in the Conclusions section.

Looking at the individual terms which make up the pressure balance in Figure 3, we can first see one of the reasons why the electrons are better balanced; for this simulation the electrons are overwhelmingly adiabatic, balancing completely with a single term, the parallel electric field.

The ions on the other hand have significant contributions to the pressure balance from numerous terms. As expected, parallel pressure is the dominant term, and non-negligible contributions are made from the parallel electric field, source, and viscosity terms. However, the largest terms are found in opposing sets of terms: the first from the electric field, $(\nabla\times\hat{\mathbf{b}})\cdot\left[-2\langle v_\parallel q\overline{\mathbf{E}}\rangle_f\right] + \hat{\mathbf{b}}\cdot\nabla\times\langle v_\parallel q\overline{\mathbf{E}}\rangle_f$, which gives a positive contribution, and the second from parallel energy flux terms, $(\nabla\times\hat{\mathbf{b}})\cdot\nabla\langle mv_\parallel^3\rangle_f + \left(\hat{\mathbf{b}}\times\nabla B/B\right)\cdot\nabla\langle 0.5 mv_\parallel v_\perp^2\rangle_f$, which gives a negative contribution. Combined these give a large net negative contribution to the pressure balance, which overcomes the positive slope of the parallel pressure term, leading to the flattening out in regions away from the divertor in Figure 2, which bring the pressure balance back to the unity level.

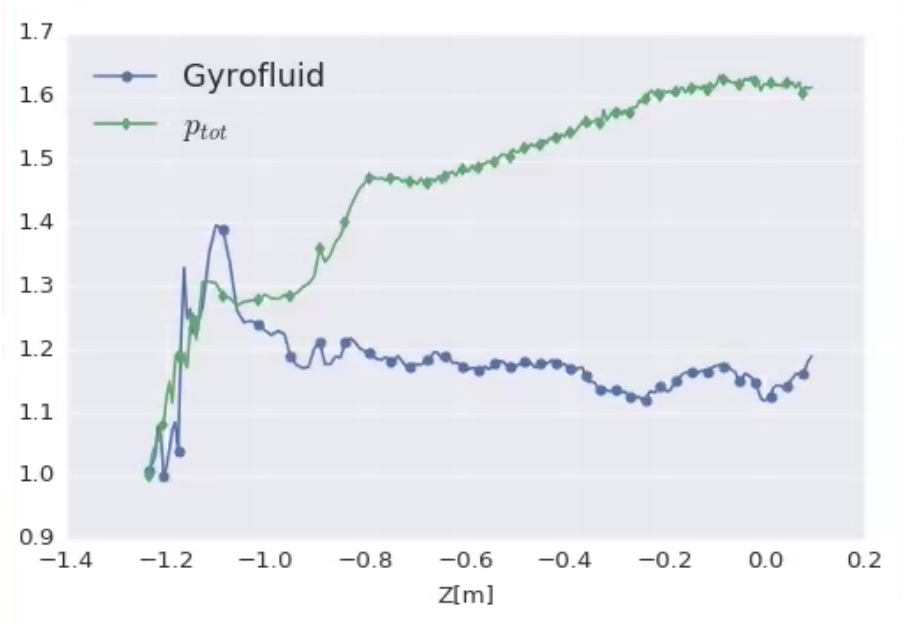

Figure 2: *Pressure balance (Equation 5) for a near-SOL flux surface (labelled "gyrofluid"; in blue). The green p_{tot} line shows for comparison the large deviation from constant pressure along the flux surface.*

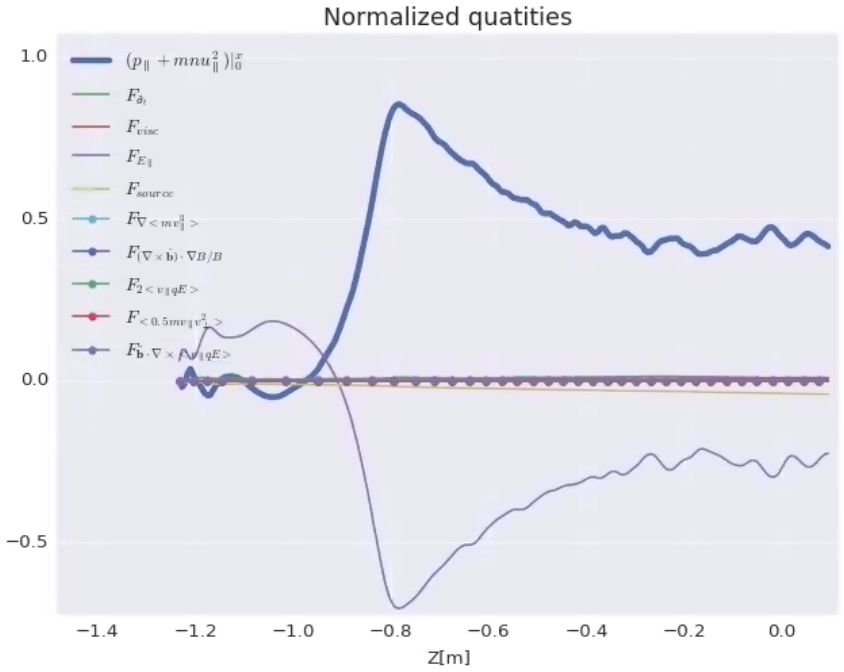

Figure 3: *Individual terms from the electron pressure balance (Equation 5) for a near-SOL flux surface*

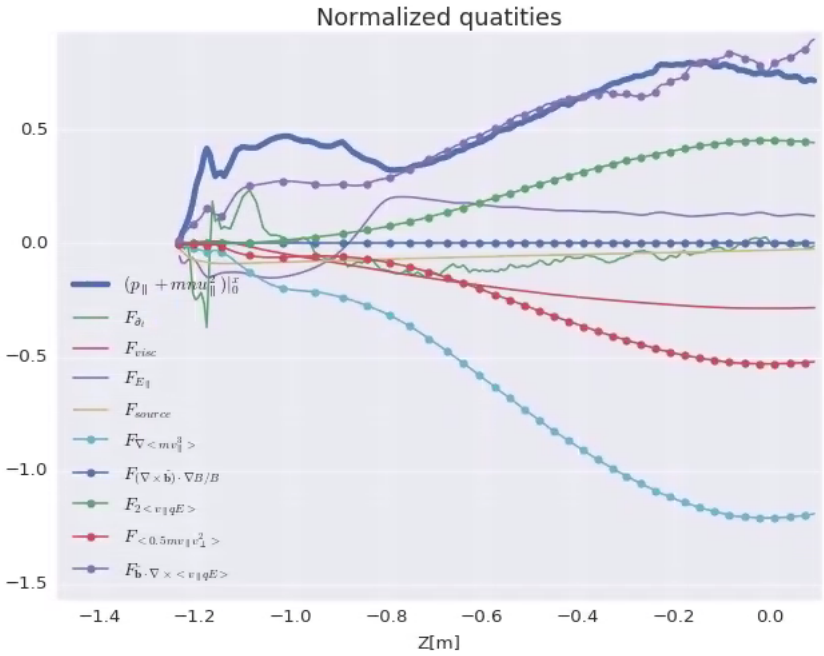

Figure 4: *Individual terms from the ion pressure balance (Equation 5) for a near-SOL flux surface*

5. Conclusions

A gyrofluid parallel momentum equation has been derived from the XGCa gyrokinetic equations of motion, for use in interpreting the relative importance of terms in setting the pressure balance in the SOL. As was shown, for this discharge the electrons are dominantly adiabatic in the SOL, while the ions have significant contributions from radial flux into/out of the flux surface volume of parallel energy flux, and due to $E \times B$ motion. Accounting for all terms brings the ion (and hence total) pressure balance much closer to the expected unity level.

Future work will focus on determining why the pressure balance isn't *completely* at unity, as would be expected since this gyrofluid equation is based directly on the equations of motion used in the XGCa code. The main issue to investigate is the numerical integration in regions near the X-point, where the small B_θ leads to a very long connection length, which with any noise in the signals may cause deviations. In general, numerical issues, including in the post-processesing and/or noisy data, certainly need to be further assessed, especially when balancing large terms with opposite signs. Because of the higher order moments (e.g. energy flux), grid resolution tests would ensure these moments are calculated accurately. Additionally, further improvements to XGCa algorithms for source handling (especially wall source) and SOL electric potential solver may provide some benefits, though aren't foreseen to make up for this difference.

Acknowledgments

The main author would like to thank Greg Hammett for helpful discussions. This material is based upon work supported by the U.S. Department of Energy, Office of Science, Office of Fusion Energy Sciences, This work supported by the US Department of Energy under DE-AC02-09CH11466, DE-AC05-00OR22725, and DE-FC02-04ER54698.

References

[1] V. Kotov and D. Reiter, Two-point analysis of the numerical modelling of detached divertor plasmas, Plasma Phys. Control. Fusion, **51**, 115002 (2009)

[2] P. C. Stangeby, Basic physical processes and reduced models for plasma detachment, Plasma Phys. Control. Fusion, **60**, 044022 (2018)

[3] P. Stangeby, *The Plasma Boundary of Magnetic Fusion Devices*, Institute of Physics Publishing, Bristol (2000)

[4] J. L. Luxon, T. C. Simonen et al., Overview of the DIII-D Fusion Science program, Fusion Sci. Technol., **48**, 807 (2005)

[5] R. Churchill, J. Canik et al., Kinetic simulations of scrape-off layer physics in the DIII-D tokamak, Nucl. Mater. Energy, **12**, 978 (2017)

[6] R. Churchill, J. Canik et al., Total fluid pressure imbalance in the scrape-off layer of tokamak plasmas, Nucl. Fusion, **57**, 046029 (2017)

[7] R. Hager and C. S. Chang, Gyrokinetic neoclassical study of the bootstrap current in the tokamak edge pedestal with fully non-linear Coulomb collisions, Phys. Plasmas, **23**, 042503 (2016)

[8] S. Ku, R. M. Churchill et al., Electrostatic gyrokinetic simulation of global tokamak boundary plasma and the generation of nonlinear intermittent turbulence (2017)

[9] R. Churchill, C. Chang et al., On pressure balance in a low collisionality tokamak scrape-off layer, Bull. Am. Phys. Soc., **Volume 62, Number 12** (2017)

[10] A. Chankin and P. Stangeby, Particle and parallel momentum balance equations with inclusion of drifts, for modelling strong- to weakly-collisional edge plasmas, Nucl. Fusion, **46**, 975 (2006)

[11] G. W. Hammett and F. W. Perkins, Fluid moment models for Landau damping with application to the ion-temperature-gradient instability, Phys. Rev. Lett., **64**, 3019 (1990)

[12] M. A. Beer, G. W. Hammett et al., Gyrofluid simulations of turbulence suppression in reversed-shear experiments on the Tokamak Fusion Test Reactor, Phys. Plasmas, **4**, 1792 (1997)

[13] P. B. Snyder, "Gyrofluid Theory and Simulation of Electromagnetic Turbulence and Transport in Tokamak Plasmas", PhD thesis (1999), URL `https://w3.pppl.gov/ hammett/gyrofluid/papers/1999/thesis.pdf`

[14] W. Dorland and G. W. Hammett, Gyrofluid turbulence models with kinetic effects, Phys. Fluids B Plasma Phys., **5**, 812 (1993)